Land Surface Heterogeneity and High-resolution Retrievals of L-band VOD and Soil Permittivity over the Arctic Boreal Forest and Permafrost

Divya Kumawat, Lun Gao
Ardeshir Ebtehaj

Mike Schwank, JP Wigneron, and Xiaojun Li

Saint Anthony Falls Laboratory
Department of Civil, Environmental and Geo- Engineering
University of Minnesota
October, 2023

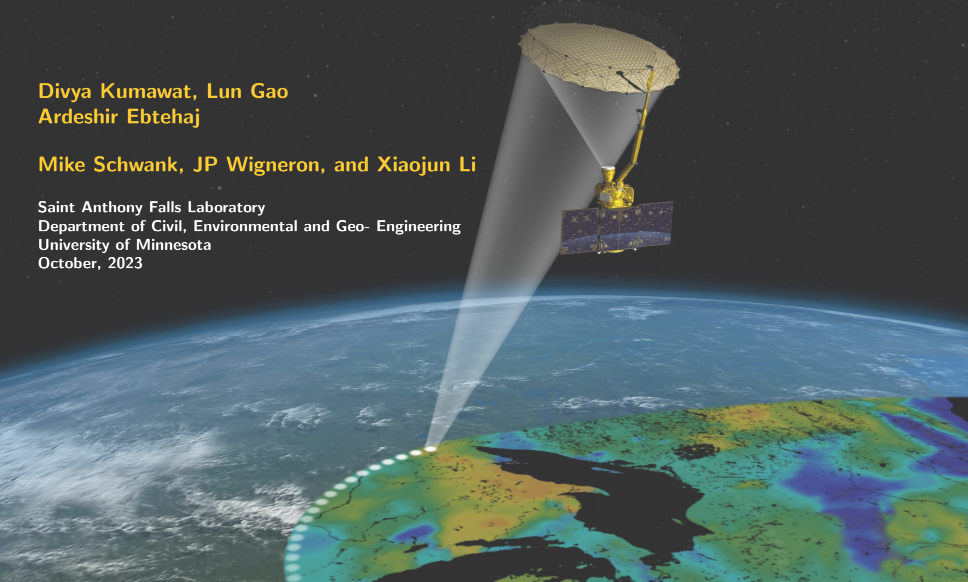

Outline

High-resolution SMAP Retrievals

- A physical or a data-driven problem?

$$SM = f(\mathbf{x})$$

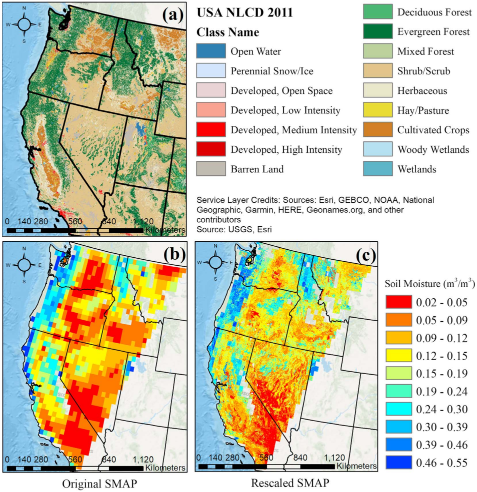

Abbaszadeh et al., 2019, Downscaling SMAP ..., https://doi.org/10.1029/2018WR023354.

Constrained Multi-Channel Algorithm (CMCA)

- Accounting for slow changes of VOD in time

$$\psi_t^* = \underset{\psi_t}{\text{argmin}} \sum_{k=1}^{K} \sum_{t=0}^{T} \|\mathbf{E}_{kt}^{-1/2}[\mathbf{e}_{kt}^p - f_{\tau-\omega}(\psi_t)]\|_2^2 + S(\psi_t) \text{ subject to } \psi_t^l \preceq \psi_t \preceq \psi_t^u$$

$$S(\psi_t) = \lambda_0 \|\theta_t^p\|_2^2 + \sum_{i=1}^{n} \lambda_i \|\mathbf{D}_i \tau_t\|_2^2$$

- Porosity at 1 km (Miller and White, 1998)

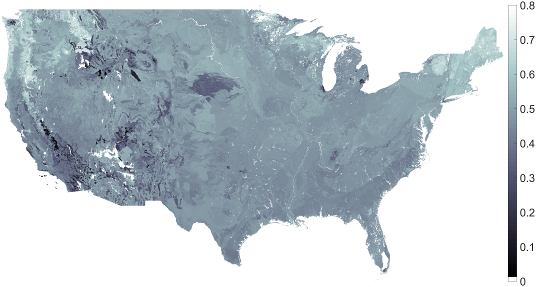

Gao L., M. Sadeghi, A. Ebtehaj (2020), https://doi.org/10.1016/j.rse.2020.111662

Constrained Multi-Channel Algorithm (CMCA)

- Accounting for slow changes of VOD in time

$$\psi_t^* = \underset{\psi_t}{\text{argmin}} \sum_{k=1}^{K} \sum_{t=0}^{T} \|\mathbf{E}_{kt}^{-1/2}[\mathbf{e}_{kt}^{p} - f_{\tau-\omega}(\psi_t)]\|_2^2 + S(\psi_t) \text{ subject to } \psi_t^l \preceq \psi_t \preceq \psi_t^u$$

$$S(\psi_t) = \lambda_0 \|\theta_t^p\|_2^2 + \sum_{i=1}^{n} \lambda_i \|\mathbf{D}_i \tau_t\|_2^2$$

- Clay fraction at 1 km (Miller and White, 1998)

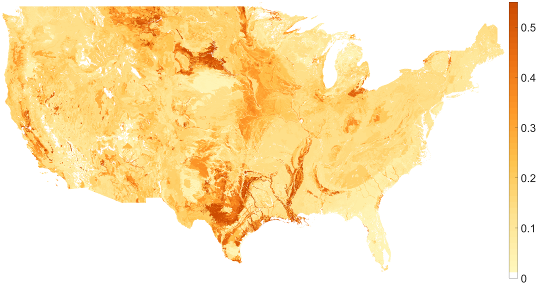

Constrained Multi-Channel Algorithm (CMCA)

- Accounting for slow changes of VOD in time

$$\psi_t^* = \underset{\psi_t}{\text{argmin}} \sum_{k=1}^{K} \sum_{t=0}^{T} \|\mathbf{E}_{kt}^{-1/2}[\mathbf{e}_{kt}^p - f_{\tau-\omega}(\psi_t)]\|_2^2 + S(\psi_t) \ \text{ subject to } \ \psi_t^l \preceq \psi_t \preceq \psi_t^u$$

$$S(\psi_t) = \lambda_0 \|\theta_t^p\|_2^2 + \sum_{i=1}^{n} \lambda_i \|\mathbf{D}_i \tau_t\|_2^2$$

- NLDAS 2006–2015 (12.5 km) and MODIS VOD data from 2000–2016 (1 km)

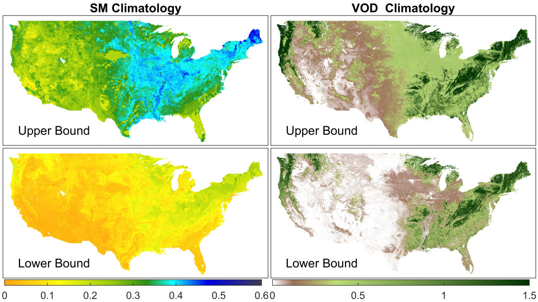

SMAP Retrievals

- SM snapshot retrievals – Feb 15, 2016

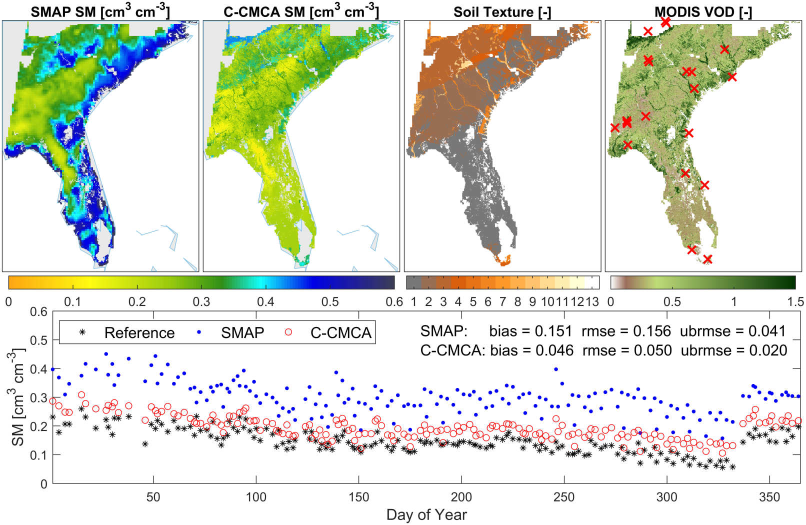

SMAP Retrievals

- SM monthly retrievals in 2016

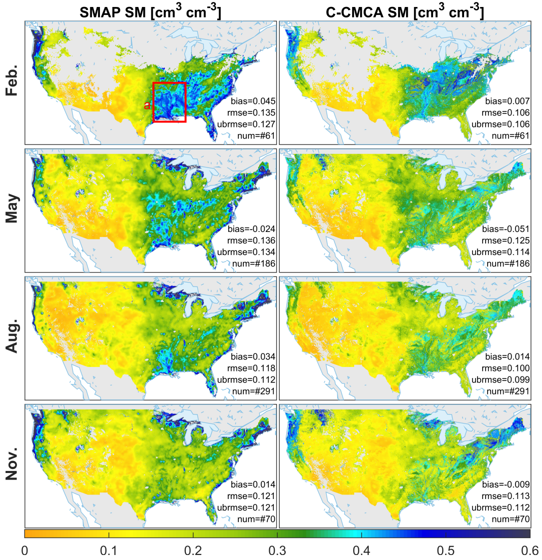

SMAP Retrievals

- SM monthly retrievals in February 2016

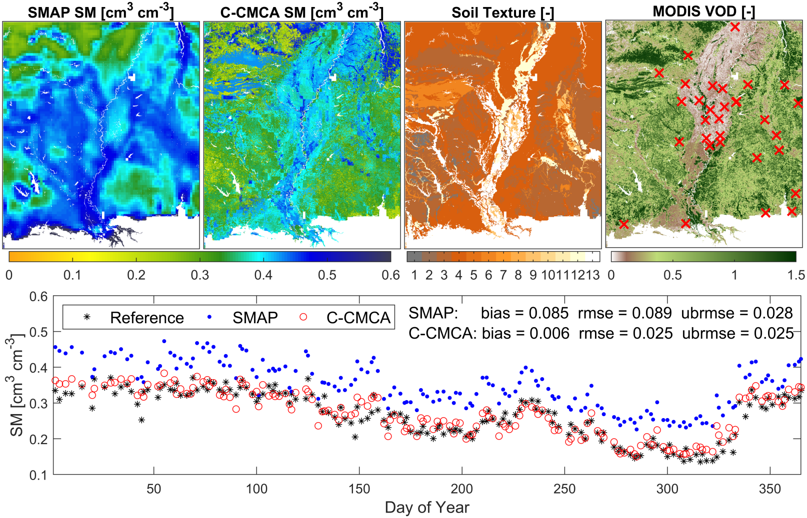

Soil Moisture below Snowpack

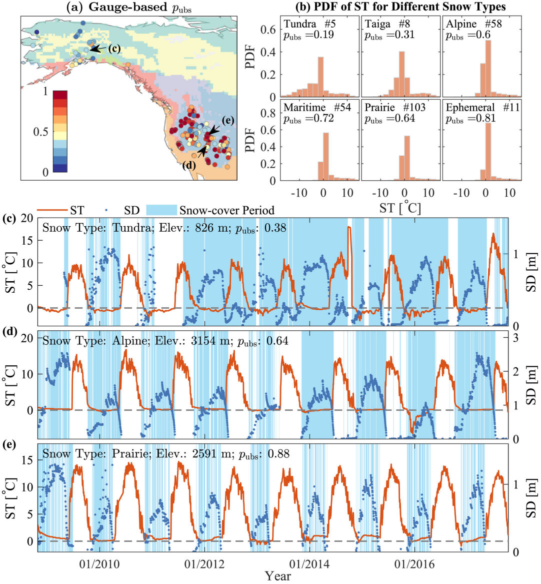

Soil-Snow-Canopy Radiative Transfer Model in L-band

$$Tb^p = \overbrace{T_g e^p \gamma_v}^{(1)} + \overbrace{T_c(1-\omega)(1-\gamma_v)}^{(2)} + \overbrace{T_c(1-\omega)(1-\gamma_v) r^p \gamma}^{(3)}$$

- e^p: effective emissivity of soil-snow system
- r^p: effective reflectivity of soil-snow system
- T_g: ground temperature
- T_c: canopy temperature.
- γ_v: vegetation transmissivity.
- ω: vegetation single scattering albedo.

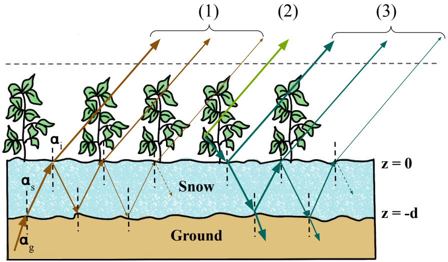

Kumawat D., M. Olyaei, L. Gao, A. Ebtehaj, Passive Microwave Retrieval of Soil Moisture below Snowpack at L-band using SMAP Observations, IEEE Trans. on Geosci. and Remote Sens., DOI:10.1109/TGRS.2022.3216324.

Soil-Snow-Canopy Radiative Transfer Model in L-band

$$r^p_{\rm coh} = \left| \frac{\xi^p_{\rm cs} + \tilde{\xi}^p_{\rm sg}\, e^{-2\gamma_{\rm s} d_{\rm s} \cos\alpha_{\rm s}}}{1 + \xi^p_{\rm cs}\,\tilde{\xi}^p_{\rm sg}\, e^{-2\gamma_{\rm s} d_{\rm s} \cos\alpha_{\rm s}}} \right|^2 \quad \text{and} \quad e^p_{\rm coh} = 1 - \left| \frac{\tilde{\xi}^p_{\rm sg} + \xi^p_{\rm cs}\, e^{-2\gamma_{\rm s} d_{\rm s} \cos\alpha_{\rm s}}}{1 + \xi^p_{\rm cs}\,\tilde{\xi}^p_{\rm sg}\, e^{-2\gamma_{\rm s} d_{\rm s} \cos\alpha_{\rm s}}} \right|^2,$$

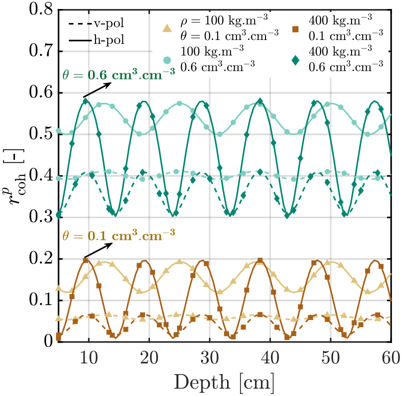

$$r^p_{\rm inc} = 1 + \mathrm{sgn}(|\xi^p_{cs}||\tilde{\xi}^p_{sg}| - 1)\, \frac{|\xi^p_{cs}|^2 + |\tilde{\xi}^p_{sg}|^2 - |\xi^p_{cs}|^2|\tilde{\xi}^p_{sg}|^2 - 1}{|\xi^p_{cs}|^2|\tilde{\xi}^p_{sg}|^2 - 1}$$

Retrieval of High-latitude VOD and Ground Permittivity

- SMAP Orbit: 23 Jan 2017

$$\phi^* = \underset{\phi}{\text{argmin}} \sum_p \left(\mathbf{y}^p_{T_B} - f^p(\boldsymbol{\phi}) \right)^2 + \mu(\tau - \tau_0)^2$$

$$\text{subject to} \quad \boldsymbol{\phi}_l \leq \boldsymbol{\phi} \leq \boldsymbol{\phi}_u,$$

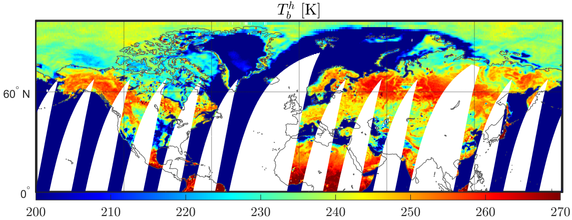

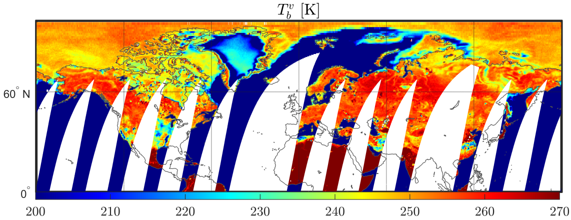

Retrieval of High-latitude VOD and Ground Permittivity

- VOD retrievals

$$\phi^* = \underset{\phi}{\text{argmin}} \sum_p \left(\mathbf{y}^p_{T_B} - f^p(\phi) \right)^2 + \mu(\tau - \tau_0)^2$$

$$\text{subject to} \quad \boldsymbol{\phi}_l \leq \boldsymbol{\phi} \leq \boldsymbol{\phi}_u,$$

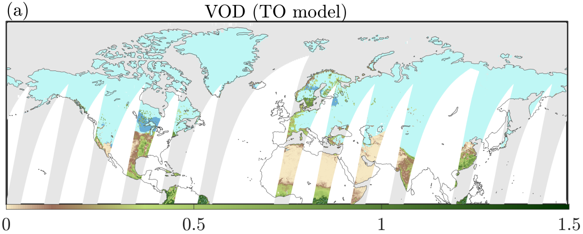

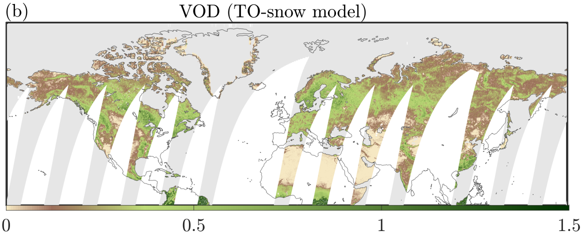

Retrieval of High-latitude VOD and Ground Permittivity

- Soil permittivity retrievals

$$\phi^* = \underset{\phi}{\text{argmin}} \sum_p \left(\mathbf{y}_{T_B}^p - f^p(\boldsymbol{\phi}) \right)^2 + \mu(\tau - \tau_0)^2$$

$$\text{subject to} \quad \boldsymbol{\phi}_l \le \boldsymbol{\phi} \le \boldsymbol{\phi}_u,$$

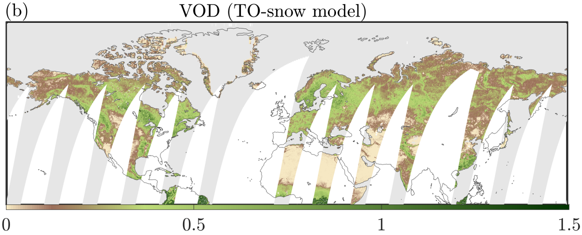

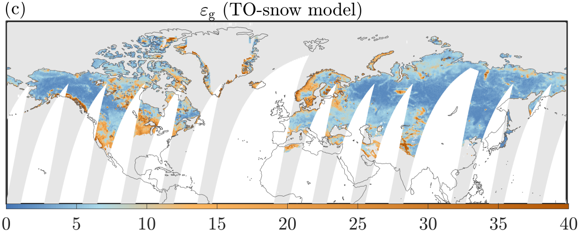

Retrieval of High-latitude VOD and Ground Permittivity

- Boreal forests with continuous (Region A) and sporadic permafrost (Region B)

$$\phi^* = \underset{\phi}{\text{argmin}} \sum_p \left(\mathbf{y}^p_{T_B} - f^p(\phi) \right)^2 + \mu(\tau - \tau_0)^2$$

$$\text{subject to} \quad \boldsymbol{\phi}_l \leq \boldsymbol{\phi} \leq \boldsymbol{\phi}_u,$$

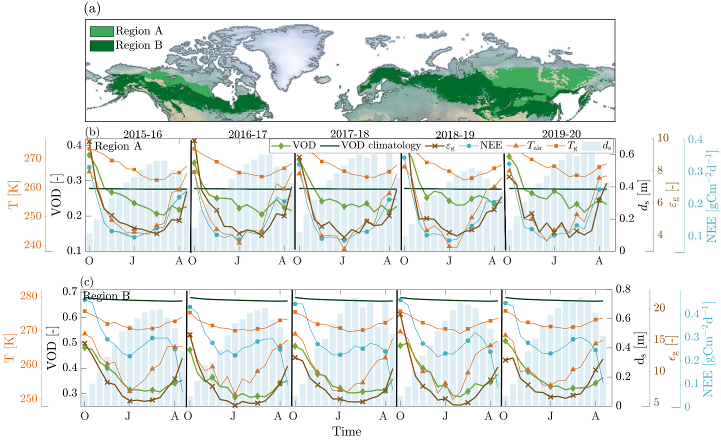

Retrieval of High-latitude VOD and Ground Permittivity

- FLUXCOM NEE in 01/23/17 and VOD.

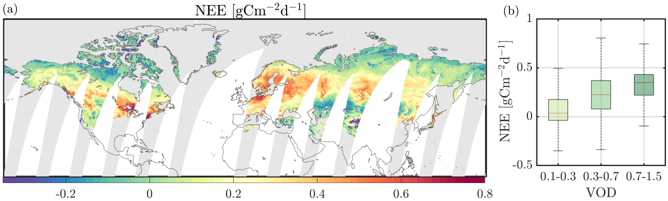

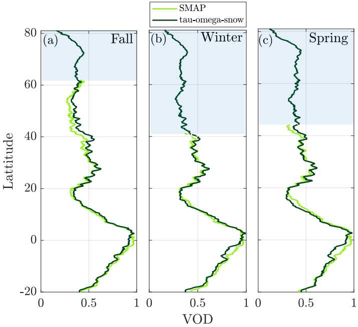

A new dataset, all SMAP daily orbits (2015–2020) at https://github.com/aebtehaj/SM-Snow-L-band

Arctic Freeze-Thaw Dynamics

$$Tb_w^p = T_w e_{is}^p \Longrightarrow Tb^p = f_w Tb_w^p + (1 - f_w) Tb_g^p$$

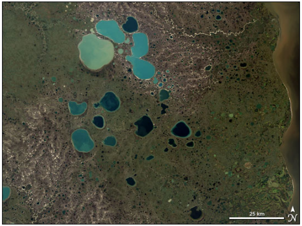

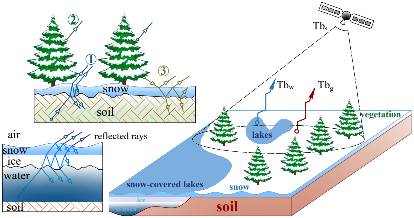

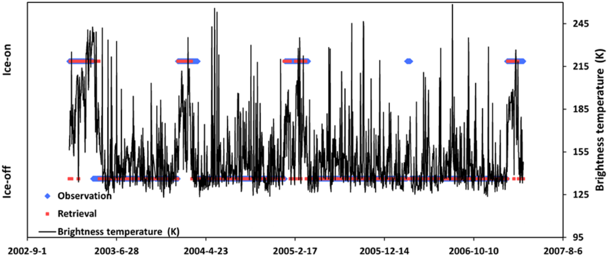

Arctic Freeze-Thaw Dynamics

$$Tb_w^p = T_w e_{is}^p \Longrightarrow Tb^p = f_w Tb_w^p + (1 - f_w) Tb_g^p$$

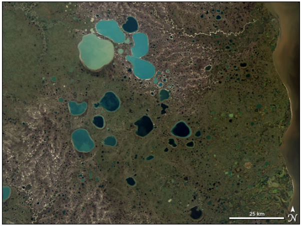

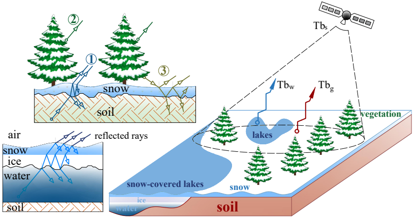

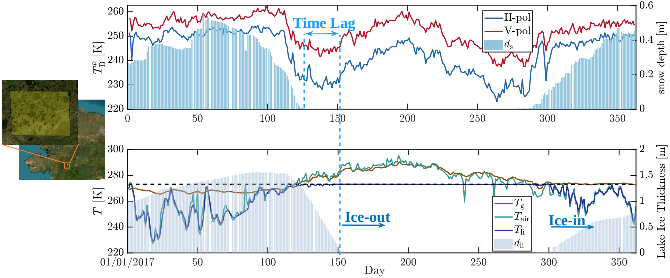

Arctic Freeze-Thaw Dynamics

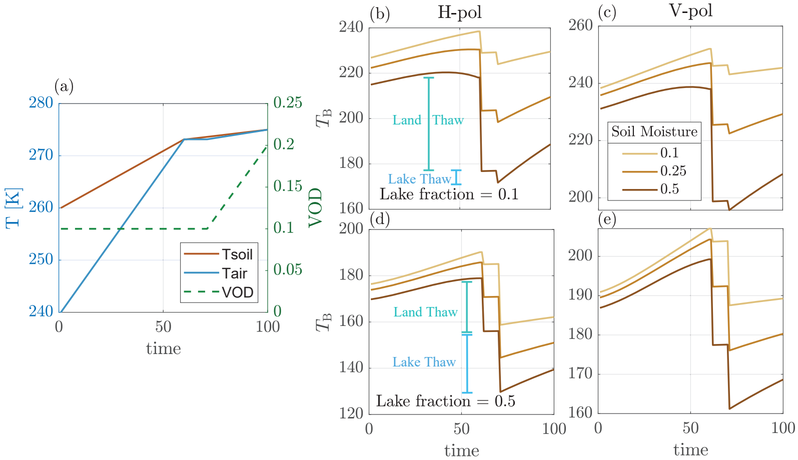

Arctic Freeze-Thaw Dynamics

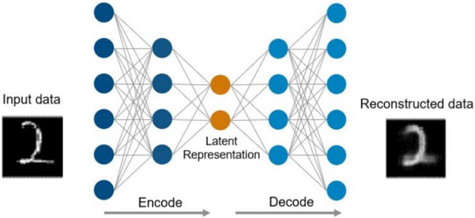

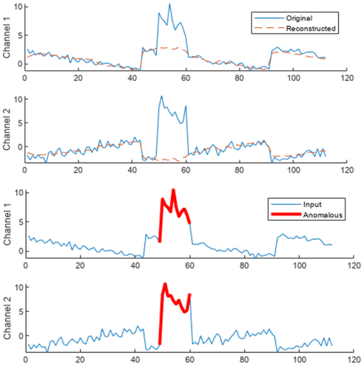

Arctic Freeze-Thaw Dynamics

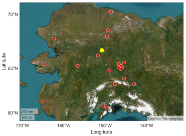

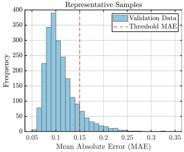

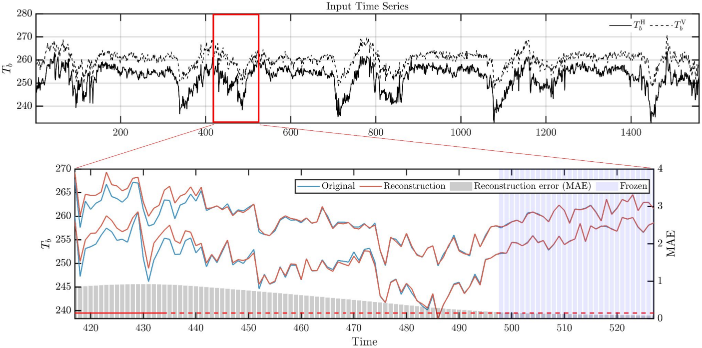

Arctic Freeze-Thaw Dynamics

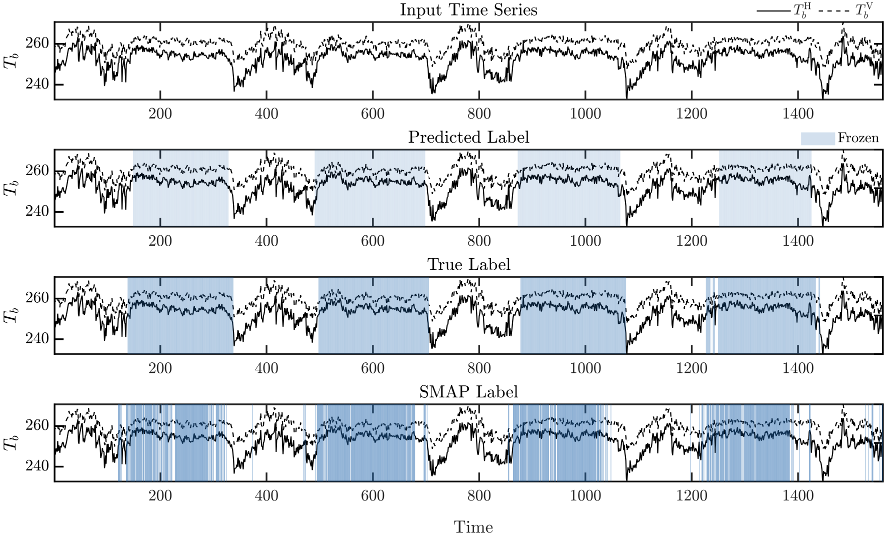

Methane Ebullition Flux

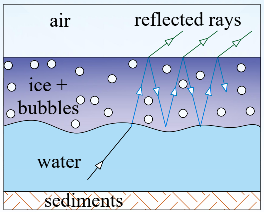

$$\epsilon_m = \epsilon_i + \frac{3v_b\epsilon_i(\epsilon_b - \epsilon_i)}{(2\epsilon_i + \epsilon_b) - v_b(\epsilon_b - \epsilon_i)} \text{(Tinga-Voss-Blossey)}$$

Methane Ebullition Flux

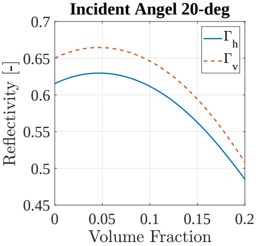

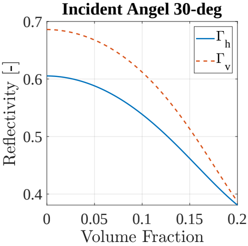

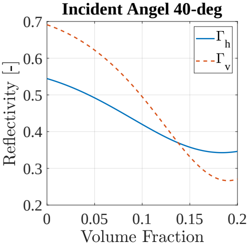

$$\epsilon_m = \epsilon_i + \frac{3v_b\epsilon_i(\epsilon_b - \epsilon_i)}{(2\epsilon_i + \epsilon_b) - v_b(\epsilon_b - \epsilon_i)} \text{(Tinga-Voss-Blossey)}$$

Summary

- Key ancillary variables that directly inform the RT model (e.g., clay fraction) can improve retrieval resolution.
- Not accounting for the effect of snow will lead to an overestimation of soil relative permittivity and VOD over the Arctic lands.
- Quantify NEE in wintertime when snow and ice cover the ground
- With 10×10 km resolution, we can estimate the ice phenology of Arctic lakes greater than 3×3 km.
- Methane ebullition flux to better understand the contribution of thawing permafrost on global warming.
- L-band PMW retrieval of active layer ice and carbon content?

Summary

- Key ancillary variables that directly inform the RT model (e.g., clay fraction) can improve retrieval resolution.
- Not accounting for the effect of snow will lead to an overestimation of soil relative permittivity and VOD over the Arctic lands.
- Quantify NEE in wintertime when snow and ice cover the ground
- With 10×10 km resolution, we can estimate the ice phenology of Arctic lakes greater than 3×3 km.
- Methane ebullition flux to better understand the contribution of thawing permafrost on global warming.
- L-band PMW retrieval of active layer ice and carbon content?

Summary

- Key ancillary variables that directly inform the RT model (e.g., clay fraction) can improve retrieval resolution.
- Not accounting for the effect of snow will lead to an overestimation of soil relative permittivity and VOD over the Arctic lands.
- Quantify NEE in wintertime when snow and ice cover the ground
- With 10×10 km resolution, we can estimate the ice phenology of Arctic lakes greater than 3×3 km.
- Methane ebullition flux to better understand the contribution of thawing permafrost on global warming.
- L-band PMW retrieval of active layer ice and carbon content?

Summary

- Key ancillary variables that directly inform the RT model (e.g., clay fraction) can improve retrieval resolution.
- Not accounting for the effect of snow will lead to an overestimation of soil relative permittivity and VOD over the Arctic lands.
- Quantify NEE in wintertime when snow and ice cover the ground
- With 10×10 km resolution, we can estimate the ice phenology of Arctic lakes greater than 3×3 km.
- Methane ebullition flux to better understand the contribution of thawing permafrost on global warming.
- L-band PMW retrieval of active layer ice and carbon content?

Summary

- Key ancillary variables that directly inform the RT model (e.g., clay fraction) can improve retrieval resolution.
- Not accounting for the effect of snow will lead to an overestimation of soil relative permittivity and VOD over the Arctic lands.
- Quantify NEE in wintertime when snow and ice cover the ground
- With 10×10 km resolution, we can estimate the ice phenology of Arctic lakes greater than 3×3 km.
- Methane ebullition flux to better understand the contribution of thawing permafrost on global warming.
- L-band PMW retrieval of active layer ice and carbon content?

Summary

- Key ancillary variables that directly inform the RT model (e.g., clay fraction) can improve retrieval resolution.
- Not accounting for the effect of snow will lead to an overestimation of soil relative permittivity and VOD over the Arctic lands.
- Quantify NEE in wintertime when snow and ice cover the ground
- With 10×10 km resolution, we can estimate the ice phenology of Arctic lakes greater than 3×3 km.
- Methane ebullition flux to better understand the contribution of thawing permafrost on global warming.
- L-band PMW retrieval of active layer ice and carbon content?